Available online at BCREC website: https://bcrec.id

Bulletin of Chemical Reaction Engineering & Catalysis, 18 (3) 2023, 460-472

Research Article

Biochar-Modified Layered Double Hydroxide for Highly Efficient on Phenol Adsorption

Amri Amri[1], Rezonsi Rezonsi[1], Nur Ahmad[1], Tarmizi Taher[2], Neza Rahayu Palapa[1], Risfidian Mohadi[1,3], Aldes Lesbani[1,3,*]

[1]Research Center of Inorganic Materials and Coordination Complexes, Universitas Sriwijaya, Palembang, 30139, Indonesia.
[2]Department of Environmental Engineering, Faculty of Mathematics and Natural Sciences, Institut Teknologi Sumatera, Lampung, 35365, Indonesia.
[3]Master Program of Material Science, Graduate School Universitas Sriwijaya, Palembang, 30139, Indonesia.

Received: 13th August 2023; Revised: 21st September 2023; Accepted: 21st September 2023
Available online: 26th September 2023; Published regularly: October 2023

Abstract

All activities require drinking water. The existence of waste makes water unfit for consumption. Phenol waste is one example of waste that is often found. The toxic and corrosive nature of phenol is very dangerous for life, so its presence must be considered. The adsorption process was carried out using NiAl and ZnAl layered double hydroxides composites with biochar to eliminate the presence of phenol waste The adsorption process was carried out using NiAl and ZnAl layered double hydroxydes materials which were composited with biochar to eliminate the presence of phenol waste. NiAl-Biochar and ZnAl-Biochar composites were successfully prepared, as determined by XRD, FTIR, SEM, and BET analyses. NiAl layered double hydroxide surface area grew from 92.683 to 438.942 m^2/g while ZnAl layered double hydroxide surface area increased from 9.621 to 58.461 m^2/g. pHpzc of material is between 5.1 and 9.4. Optimal pH of NiAl and ZnAl layered double hydroxide is 3, optimum pH of NiAl-Biochar and ZnAl-Biochar is 5, and optimum pH of Biochar is 7. All kinetic and isotherm models for all materials were pseudo-second-order and Freundlich, respectively. NiAl-Biochar and ZnAl-Biochar have maximal adsorption capacities of 74.62 mg/g and 52.91 mg/g, respectively. The material's reusability indicates that NiAl-Biochar has superior qualities and may be reused for up to five cycles, followed by ZnAl-Biochar, NiAl layered double hydroxide, ZnAl layered double hydroxide, and Biochar.

Keywords: Biochar; Phenol; Adsorption; Layered double hydroxide

How to Cite: A. Amri, R. Rezonsi, N. Ahmad, T. Taher, N.R. Palapa, R. Mohadi, A. Lesbani (2023). Biochar-Modified Layered Double Hydroxide for Highly Efficient on Phenol Adsorption. *Bulletin of Chemical Reaction Engineering & Catalysis*, 18(3), 460-472 (doi: 10.9767/bcrec.19898)

Permalink/DOI: https://doi.org/10.9767/bcrec.19898

1. Introduction

Water is one of the main needs for carrying out all human activities. Healthy drinking water must meet the chemical, physical, and microbiological requirements. The presence of household waste, industrial waste, and organic waste makes drinking water suitable for consumption very difficult to obtain in big cities [1]. Phenol is one of the wastes generated from the plastic, paint, pharmaceutical, oil and gas, and ceramic industries. In addition, phenol waste is also generated through household waste, namely from floor cleaning residue. Because of its toxic and corrosive properties, phenol is extremely hazardous to life [2].

There are many ways to remove phenolic compounds, including using electrocoagulation,

* Corresponding Author.
Email: aldeslesbani@pps.unsri.ac.id (A. Lesbani)

biodegradation, photochemical, Fenton, and adsorption methods [3–5]. However, the adsorption method is a method that is very commonly used because it is easy to operate, low cost, and has high efficiency [6]. Various kinds of adsorbents are used in phenol adsorption, including biochar [7], clay [8], graphite [9], and layered double hydroxide [10].

Layered double hydroxide (LDH) has a unique property of flexibility, where the interlayer anions can be replaced according to the application of the LDH [11]. In addition, LDH has a large surface, so it is very useful in adsorption but has poor structural stability, so it is easy to peel off during application, which results in reduced efficiency in reuse in the adsorption process [12,13]. Therefore, it is necessary to add a supporting material in order to improve the structure so that it has better adsorption ability. There are many methods that can be used to synthesize LDH including ion exchange, sol-gel, calcination-hydration, and coprecipitation methods [14,15]. However, the coprecipitation method is the most widely used method because it is simple, low cost and does not use high temperatures [16,17].

There are various types of carbon-based materials that can be applied as support materials in improving the structure of LDH, namely graphite, charcoal, chitosan, and biochar [18–21]. Biochar (BC) is a material produced from the decomposition of organic matter which has advantages including being friendly to the environment, easy to manufacture at low cost, abundant availability of raw materials, and has a porous structure which is very helpful in the adsorption process [22,23].

Several studies have investigated the usefulness of LDH composited with carbon-based materials for the adsorption of various types of waste. Research conducted by Normah *et al*. [24] improved the structure of the NiAl LDH by adding a graphite support material that could increase the adsorption capacity from 29.586 to 72.464 mg/g, and after the composite was performed, the effectiveness of the adsorption process was seen. Up to five reusability cycles did not experience a significant decrease. In addition, the addition of supporting materials to improve the structure of LDH can increase the surface area. This is evidenced by Mahgoub *et al*. [25] who added cellulose activated carbon to the layered double hydroxide material, increasing its surface area from 50.96 to 303.79 m^2/g which was very helpful in increasing the adsorption capacity. Hoang *et al*. [26] used ZnAl LDH material composited with bagasse biochar to remove tetracyclines. The results obtained showed an increase in surface area from 404.05 m^2/g in bagasse biochar to 456.39 m^2/g in ZnAl-Biochar bagasse. Another study also used LDH/biochar composite materials to remove cadmium as was done by Liao *et al*. [27]. The results indicated that the surface area of biochar increased from 71.170 m^2/g to 384.198 m^2/g, and that its adsorption capacity increased from 44.51 mg/g to 181.53 mg/g. Thus, it is required to do additional research on the creation of waste-removal materials derived from various forms of biochar and LDH.

In this study, NiAl and ZnAl layered double hydroxide materials were composited to Biochar from rice husk using co-precipitation method and then characterized using XRD, FT-IR, SEM, and BET. Determination of the adsorption capacity of phenolic compounds on various materials was observed by carrying out various influences such as pH, time, concentration and adsorption temperature as well as looking at the usability of the material in repeated use.

2. Materials and Methods

2.1 Chemicals and Instrumentation

In this work, the chemicals used are biochar by Bukata Organic Indonesia, hydrogen chloride (HCl) by Mallinckrodt, sodium carbonate (Na_2CO_3) by Merck, potassium hexacyanoferrate(III) ($K_3[Fe(CN)_6]$) by Pudak scientific, phenol solution by Sigma Aldrich, 4-aminoantipyrine ($C_{11}H_{13}N_3O$) by Loba Chemie PVT. LTD., pH 10 buffer solution by SMART-Lab Indonesia, sodium hydroxide (NaOH) by Sigma Aldrich. In addition, materials such as (nickel nitrate hexahydrate ($Ni(NO_3)_2.6H_2O$), zinc nitrate hexahydrate ($Zn(NO_3)_2.6H_2O$), and aluminum nitrate nonahydrate ($Al(NO_3)_3.9H_2O$) by Sigma Aldrich) are utilized as precursors in the production of NiAl and ZnAl LDH, respectively. The Fourier Transform Infra-Red (FTIR) type Shimadzu Prestige-21, Biobase BK-UV 1800 PC, an ultraviolet-visible spectrophotometer with a wavelength of 510 nm, the Surface Area & Pore Size Analyzer (BET) type NOVA 4200e, the SEM type Quanta-650 Oxford, and The X-Ray Diffraction (XRD) type Rigaku Miniflex-6000 are supporting tools in this study.

2.2 Synthesis of NiAl LDH

100 mL of $Ni(NO_3)_2.6H_2O$ 0.75 M and $Al(NO_3)_3.9H_2O$ 0.25 M solutions each, followed by the addition of a mixture of 0.3 M Na_2CO_3 100 mL and 50 mL of 2 M NaOH gradually.

The pH of the solution was then adjusted to 10 by adding 2 M NaOH. The resultant mixture was swirled continuously for 17 h at 80 °C. Furthermore, the samples were rinsed with distilled water, filtered and put in an oven with a temperature of 100 °C for drying.

2.3 Synthesis of ZnAl LDH

In a beaker glass, 100 mL of 0.25 M $Al(NO_3)_3.9H_2O$ solution and 100 mL of 0.75 M $Zn(NO_3)_2.6H_2O$ were added. In addition, 2 M NaOH was added to the mixture in order to lower its pH to 8. The mixture was swirled for 4 h at 80 °C. After being treated, the ZnAl LDH material was then filtered, washed, and dried.

2.4 Preparation of NiAl-BC

30 mL of each solution of 0.75 M $Ni(NO_3)_2.6H_2O$ and 0.25 M $Al(NO_3)_3.9H_2O$ were combined in a beaker, 2 M NaOH was slowly added to obtain a pH of 10, and the mixture was agitated for 1 h. In addition, 3 g of biochar are added to the mixture and mixed for three days at 80 °C. Before being heated at 100 °C, the precipitate was filtered and rinsed with deionized water.

2.5 Preparation of ZnAl-BC

30 mL of each of the solutions 0.75 M $Zn(NO_3)_2.6H_2O$ and 0.25 M $Al(NO_3)_3.9H_2O$ were combined in a beaker. Slowly adding 2 M NaOH to the mixture until the pH reached 8 and stirring for 1 h brought the pH to 8. Additionally, 3 g of biochar are added to the mixture, which is then agitated at 80°C for 72 h. The precipitate obtained was filtered and rinsed with distilled water. Furthermore, drying is carried out by placing it in the oven at a temperature of 100°C.

2.6 Performance of pH point zero charge (pHpzc)

This was done by adding 20 mL of 0.1 M NaCl solution which had been set to a pH of 2, 3, 4, 5, 6, 7, 8, 9, 10, and 11. Then 0.02 g of each adsorbent was added and stirred for 24 h. Furthermore, pH measurements were carried out after the selation stirring process to show the presence of no charge in each adsorbent by making a graph of the relationship between the initial pH and the final pH.

2.7 Adsorption of Phenol

The effect of pH, time and the effect of concentration and temperature were observed during the investigation on the phenol adsorption process. In addition, also investigated was the reusability process. The investigation was carried out by inserting 20 mL of phenol solution into a beaker and adding 0.02 g of each adsorbent. Variation of pH is done by setting pH 2-11; contact times used are 0, 5, 10, 20, 30, 40, 50, 60, 70, 90, 120, 150, 180, and 200 min; the effect of concentration and temperature is carried out with concentrations of 15, 20, 25, 30, and 35 mg/L (30-70 °C).

The solution was complexed by combining 1 mL of phenol solution, 1 mL of pH-10 buffer solution, 0.1 mL each of 8% hexacyanoferrate (III) and 2% 4-aminoantipyrine reagent, and 3 mL of distilled water in a beaker before measuring the absorbance with a UV-VIS spectrophotometer. After being homogenized, the mixture was let to stand for 15 min. The concentration was then determined by measuring the absorbance.

2.8 Desorption and Regeneration of Adsorbent on Phenol Adsorption

Desorption treatment was carried out after the adsorption process was complete. At first, adsorption was carried out as usual, using 15 mg/L of phenol solution and adding 0.02 g of adsorbent and stirring for up to 2 h. After that, the separation between the filtrate and precipitate was carried out. The precipitate is dried and a desorption process is carried out using 10 mL of distilled water which is put into an ultrasonic device to release the adsorbate attached to the adsorbent. While the filtrate is measured to determine the adsorbed concentration. The regeneration process is carried out by doing the same thing for up to five cycles.

3. Results and Discussion

3.1 Point of Zero Charge (PZC) of the Adsorbent Materials

The PZC value identifies the state of a material on the surface that has no charge or is zero. A positive charge on the surface is shown by a pH value below the PZC, and a negative charge is indicated by a pH value above the PZC [4]. The PZC chart is shown in Figure 1. Based on the PZC values obtained, the PZC values in NiAl LDH are pH 8.3, ZnAl LDH at pH 5.9, BC at pH 5.1, NiAl-BC at pH 9.4, and ZnAl-BC at pH 6.7. This identifies the neutral charge of each material.

3.2 Effect of pH

pH has a major influence on the phenol adsorption process, which can affect the nature

and structure of the adsorbate and adsorbent, causing differences in adsorption abilities [28]. Based on Figure 2, the optimal pH of NiAl LDH and ZnAl LDH is 3, the optimal pH of NiAl-BC and ZnAl-BC is 5, and the pH at BC is 7. This proves that if pH < pHpzc indicates the charge on the surface of the adsorbent is positive. According to Alminderej *et al.* [29], the presence of a positive surface on the adsorbent will increase the electrostatic force between the phenolic anions so as to increase the ability of the adsorption process. However, when the pH is high or alkaline it will cause the adsorbent to be negatively charged. Therefore, it can experience a decrease in adsorption capacity due to electrostatic repulsion between the negatively charged phenolic anions and the negatively charged adsorbent [30]. Furthermore, the optimal pH that has been obtained will be used in the adsorption process.

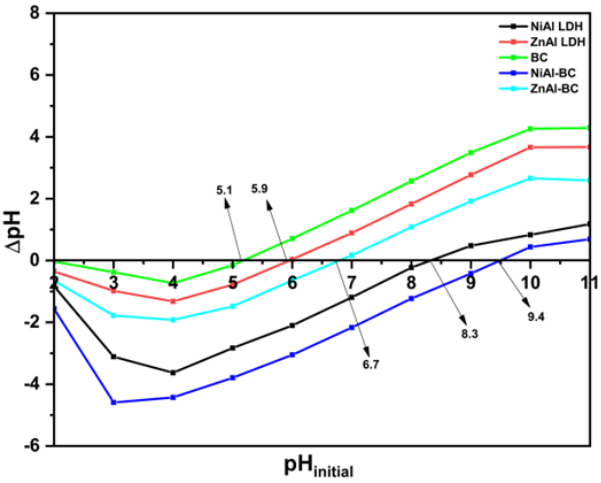

Figure 1. PZC of adsorbent materials.

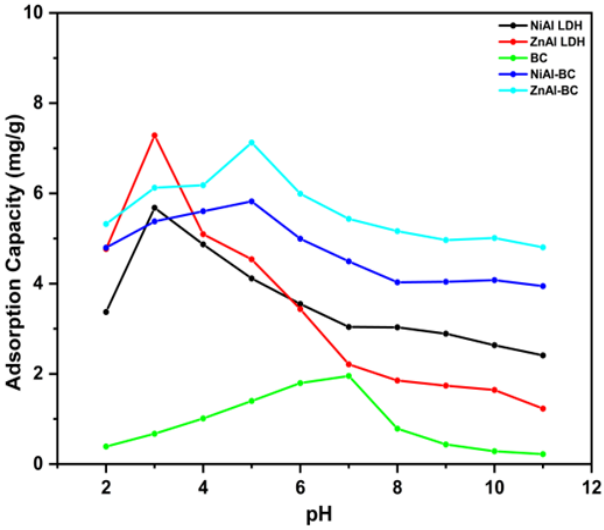

Figure 2. Effect of pH on adsorption of phenol.

3.3 Characterization of the Adsorbent Materials

Figure 3 shows the XRD patterns of NiAl LDH, ZnAl LDH, BC, NiAl-BC, and ZnAl-BC. NiAl LDH displayed a diffraction peak of 2θ = 11.74° (003); 23.33° (006); 34.5° (009); and 60.26° (110), while ZnAl LDH displayed a diffraction peak at 2θ = 11.74° (003); 23.33° (006); 34.5° (009); 39.26° (015); 60.26° (110); and 61.17° (113), both of which are characteristic peaks of LDH according to JCPDS data no. 38–0486 [31]. The diffraction peak at an angle of 2θ = 22.30° (002) is a typical pattern of biochar as a material with an amorphous structure. This is in accordance with research conducted by Prakongkep *et al.* [32] who performed XRD analysis of biochar produced a diffraction peak at an angle of 2θ = 22.50° (002). When the NiAl and ZnAl LDH were composited on biochar, there was a shift of 2θ = 11.74° (003) in a smaller direction, namely to 2θ = 10.85° (003). This is due to the addition of carbon material (biochar) to LDH [33]. In the ZnAl-BC and NiAl-BC composite materials there are diffraction peaks for each constituent material, so that it can be ascertained that the NiAl-BC and ZnAl-BC composite materials were successful.

The FTIR spectra of NiAl LDH, ZnAl LDH, BC, NiAl-BC, and ZnAl-BC are depicted in Figure 4. The strong absorption band around 1381 cm^{-1} implies that nitrate anions are present in the LDH interlayer [34]. The large absorption band near 3448 cm^{-1} indicates the presence of -OH stretching vibrations. Ravuru *et al.* [35] said that the absorption band around 3448 cm^{-1} indicates that in the LDH interlayer there are O–H vibrations in water molecules. Metal-

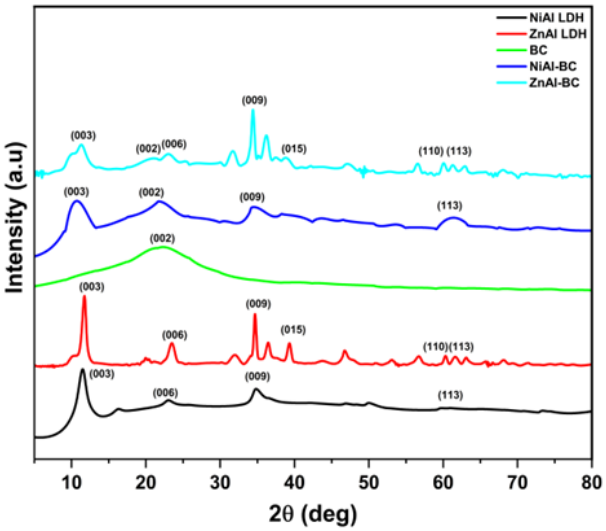

Figure 3. X-ray diffractogram of adsorbents.

oxide vibrations are indicated by absorption bands at wave numbers 748, 601, and 470 cm^{-1}. In the BC material, absorption bands at wave numbers 2931 and 1049 cm^{-1} were obtained, respectively indicating CH_2 distortion and C–O vibrations of polysaccharides. The wave numbers 1627, 1386, and 826 cm^{-1} indicate the presence of C=C bonds, C=O, and C–H stretching vibrations in aromatics. The OH stretching vibration is seen in the wave number around 3440 cm^{-1} [36]. In the composite material, it can be seen that there are additional peaks in wave numbers in the 1049 and 2931 cm^{-1} areas which indicate the presence of C–O vibration and CH_2 distortion originating from BC. This shows that the NiAl-BC and ZnAl-BC composites are successful.

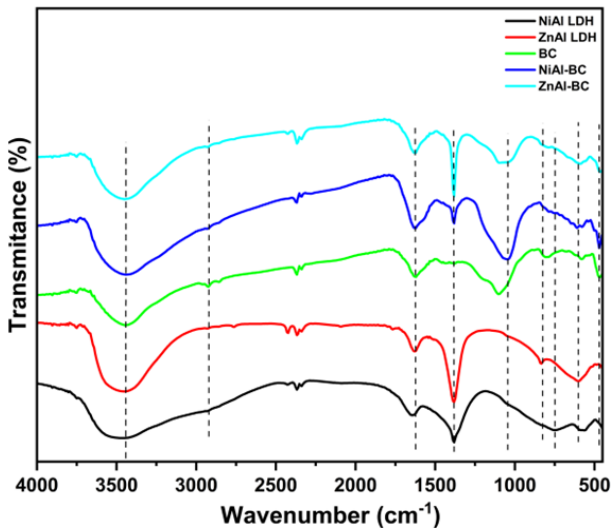

Figure 4. Fourier transfer infra-red spectrum of adsorbents

SEM images of the morphology of NiAl LDH, ZnAl LDH, BC, NiAl-BC, and ZnAl-BC can be seen in Figure 5. The NiAl-BC and ZnAl-BC composites were successfully formed, as shown in Figures 5(d) and (e). This is because the LDH surface of the NiAl-BC and ZnAl-BC composite materials is well distributed by BC particles so as to increase the surface area [37]. However, Figure 5(e) demonstrates the existence of an uneven plate-like structure with various diameters that permits BC to deposit on the LDH surface [38].

Figure 6 shows the nitrogen adsorption-desorption isotherms on NiAl LDH, ZnAl LDH, BC, NiAl-BC, and ZnAl-BC materials. The results obtained showed all type IV hysteresis loop isotherms. This states that all materials have mesoporous characteristics [39]. According to Limau Jadam *et al.* [40], monolayer adsorption occurs at low partial pressures on the type IV nitrogen adsorption-desorption isotherm, followed by multilayer adsorption growth at high partial pressures.

Using BET and BJH methods, the surface area and pore volume of NiAl LDH, ZnAl LDH, BC, NiAl-BC, and ZnAl-BC materials can be

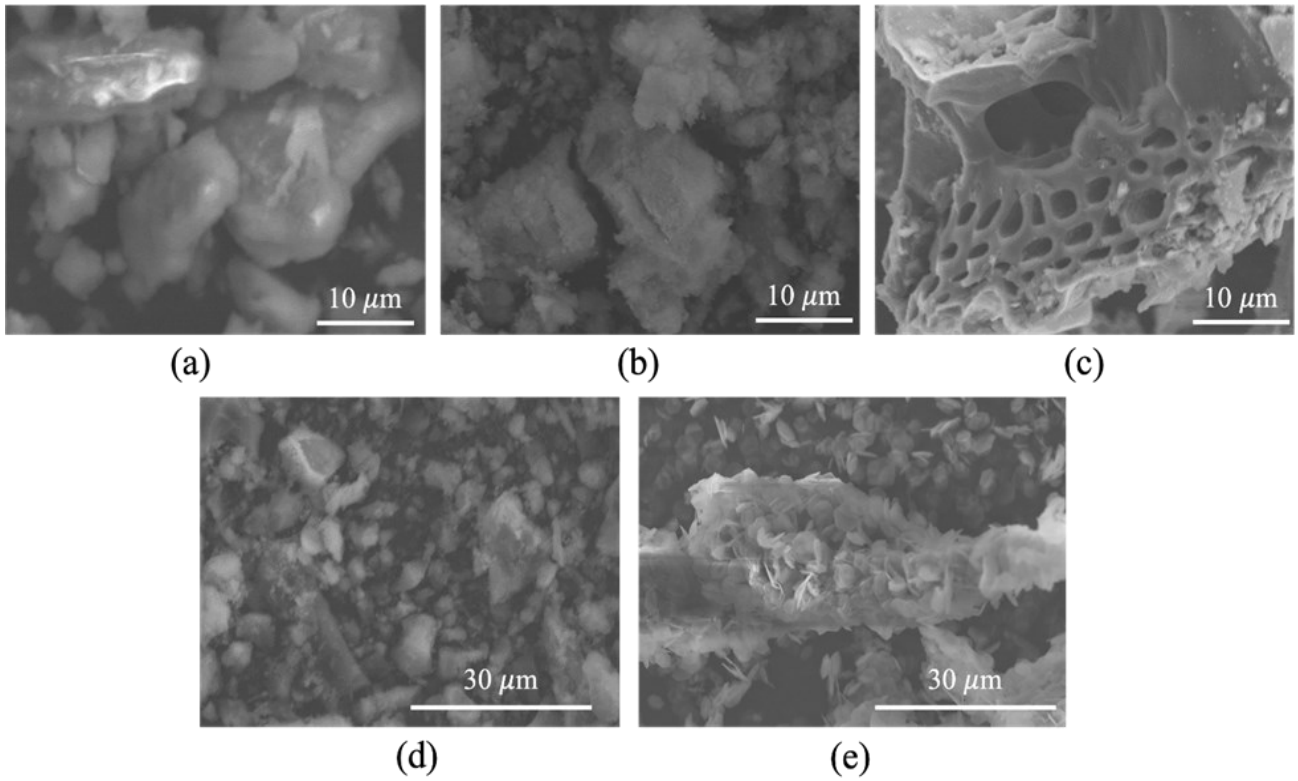

Figure 5. SEM Image of (a) NiAl LDH, (b) ZnAl LDH, (c) BC, (d) NiAl-BC, and ZnAl-BC.

determined [40]. The surface area of NiAl LDH material increased from 92.683 to 438.942 m^2/g as a result of the addition of biochar in NiAl-BC composite material. The same phenomenon also occurred in the ZnAl-BC composite material whose surface area increased to 58.461 m^2/g from 9.621 m^2/g due to the addition of BC to the ZnAl LDH material. This is in accordance with research conducted by Liao *et al*. [27] who experienced an increase in the surface area of composite materials with previous precursor materials. Therefore, it can be seen in Table 1 that the identification of the success of LDH modification with Biochar with increased surface area has been successfully carried out.

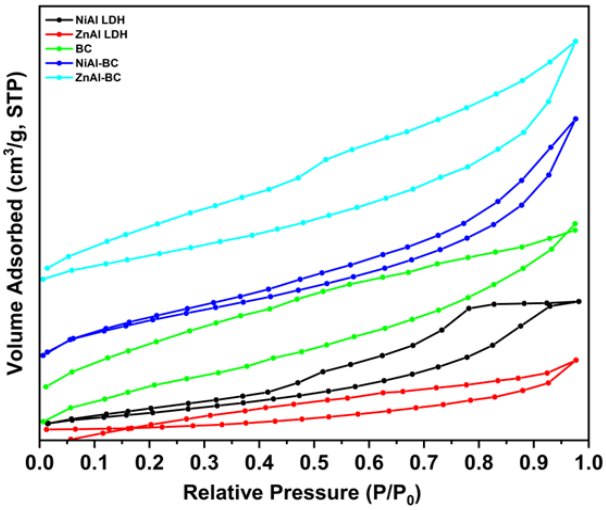

Figure 6. Graph nitrogen adsorption-desorption isotherms of adsorbents.

3.4 Effect of Time and Kinetics study

Figure 7 depicts an increase in the concentration of phenol adsorbed on NiAl-BC up to 60 min, after which the concentration tends to remain constant. The BC and ZnAl BC materials have the ability to last up to 70 min, while the ZnAl and NiAl LDH have the ability to last up to 90 min. Using pseudo-first order (PFO) and pseudo-second order (PSO) kinetic models, it is also possible to forecast the adsorption rate based on the influence of time. With the the minimum kinetic rate (k), correlation coefficient (R^2) approaching 1, and the similarity between the predicted and observed Q_e values, the kinetic model for the adsorption process may be determined. Based on the data in Table

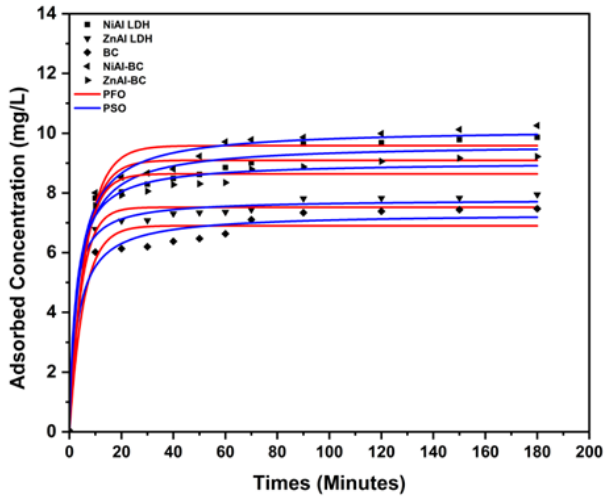

Figure 7. Adsorption kinetic model.

Table 1. Brunauer Emmet Teller of adsorbents.

Material	Surface Area (m^2/g)	Pore Size (nm), BJH	Pore Volume (cm^3/g), BJH
NiAl LDH	92.683	13.206	0.001
ZnAl LDH	9.621	12.094	0.017
BC	50.936	12.089	0.025
NiAl-BC	438.942	12.301	0.002
ZnAl-BC	58.461	12.226	0.065

Table 2. Kinetic variables models of pseudo-first- and pseudo-second-order.

kinetic model	parameter	Adsorbents				
		NiAl LDH	ZnAl LDH	BC	NiAl-BC	ZnAl-BC
pseudo first order	Qe_{exp} (mg/g)	10.113	8.167	10.78	10.555	9.436
	Qe_{calc} (mg/g)	3.459	2.117	4.103	4.102	3.557
	k_1 (min^{-1})	0.026	0.020	0.027	0.025	0.027
	R^2	0.892	0.776	0.914	0.911	0.893
pseudo second order	Qe_{exp} (mg/g)	10.113	8.167	10.78	10.555	9.436
	Qe_{calc} (mg/g)	10.341	8.453	11.062	10.846	9.653
	k_2 (min^{-1})	0.020	0.017	0.017	0.016	0.020
	R^2	0.999	0.999	0.999	0.999	0.999

2, it shows that all adsorbents follow the PSO kinetics model. According to Li *et al*. [41], the PSO kinetic model indicates that the adsorption process proceeds in two stages, with the first fast phase involving physical adsorption or ion exchange on the surface of the adsorbent and the succeeding slow phase involving mechanisms such as microprecipitation. PSO also shows that there are physicochemical interac-

Table 3. Langmuir and Freundlich kinetic models.

Adsorbent	T (°C)	Langmuir			Freundlich		
		Q_{max}	k_L	R^2	n	k_F	R^2
NiAl LDH	30	32.68	1.000	0.904	3.211	10.61	0.970
	40	45.87	0.089	0.955	2.296	7.85	0.989
	50	41.52	0.086	0.995	3.293	9.36	0.996
	60	31.25	0.539	0.903	4.993	16.61	0.974
	70	31.75	0.734	0.936	5.519	18.52	0.977
ZnAl LDH	30	24.81	0.683	0.835	8.190	16.30	0.937
	40	37.17	0.128	0.867	2.675	8,83	0.949
	50	34.48	0.182	0.875	3.315	11.04	0.947
	60	32.15	0,281	0.969	3.986	13.18	0.994
	70	31.35	0.391	0.942	4.521	14.92	0.969
BC	30	27.17	0.891	0.686	8.396	18.57	0.791
	40	27.54	1.152	0.831	9.969	19.99	0.909
	50	35.33	0.299	0.939	3.592	13.83	0.965
	60	27.93	2.435	0.886	15,570	23.23	0.973
	70	28.01	4.200	0.959	22.989	24.87	0.979
NiAl-BC	30	74.62	0.047	0.933	2.011	7.23	0.977
	40	48.54	0.104	0.968	3.011	10.57	0.992
	50	38.17	0.189	0.987	4.810	13.96	0.998
	60	35.46	0.492	0.995	4.545	17.30	0.999
	70	34.84	0.408	0.981	7.634	17.78	0.995
ZnAl-BC	30	34.96	0.195	0.830	2.996	10.65	0.917
	40	52.91	0.078	0.951	2.011	7.28	0.989
	50	31.64	0.382	0.896	4.444	14.85	0.956
	60	32.25	0.457	0.977	4.533	15.87	0.999
	70	32.05	0.606	0.989	5.028	17.47	0.993

Table 4. Maximum adsorption capacity of phenol and comparison with other researches.

Adsorbent	Q_{max} (mg/g)	Reference
Clay	10.00	[45]
Fe_3O_4/chitosan/ZIF-8	6.43	[46]
Graphene oxide	10.23	[47]
Lignite	6.22	[48]
Zeolite	34.5	[49]
Peanut shells	21.00	[50]
Chitosan/calcined eggshell	10.13	[51]
Double-network nanocomposite hydrogel	16.52	[52]
Zinc Oxide	4.69	[53]
Rice husk ash	13.98	[54]
NiAl LDH	45.87	This work
ZnAl LDH	37.17	This work
Biochar	35.33	This work
NiAl-BC	74.62	This work
ZnAl-BC	52.91	This work

tions going on during the adsorption process [42].

3.5 Effect of Isotherms and Thermodynamic Studies

Langmuir and Freundlich isotherm parameters can be seen in Table 3. Determination of isotherm parameters is carried out to determine whether the adsorption process that occurs is more dominant chemically or physically [43]. Based on the data in Table 3, all adsorbent materials follow the Freundlich isotherm model, where the value of the correlation coefficient (R^2) is closer to one. According to Budnyak *et al*. [44], the Freundlich isotherm is an adsorption process that occurs in multilayers. The maximum adsorption capacities of NiAl LDH, ZnAl LDH, BC, NiAl-BC, and ZnAl-BC were 45.87, 37.17, 35.33, 74.62, and 52.91 mg/g, respectively. Based on the data in Table 4, it shows the difference in maximum adsorption capacity between this study and other studies.

Table 5 displays adsorption thermodynamic parameters such as ΔH, ΔS, and ΔG. Based on the data obtained, the value of ΔH is positive, which describes endothermic adsorption. The enthalpy values (ΔH) of ZnAl LDH and ZnAl-BC show smaller values than the enthalpy values of BC, NiAl LDH, and NiAl-BC. The smaller enthalpy value indicates a better physisorption adsorption process. A small entropy value (ΔS) indicates a small degree of freedom. ΔG is negative, ensuring that the adsorption process occurs spontaneously. According to [48], a value of ΔG less than 20 kJ/mol indicates adsorption that occurs by physisorption. The types of bonds that occur in physisorption are hydrogen bonds, π-π interactions, and electrostatic interactions [55,56].

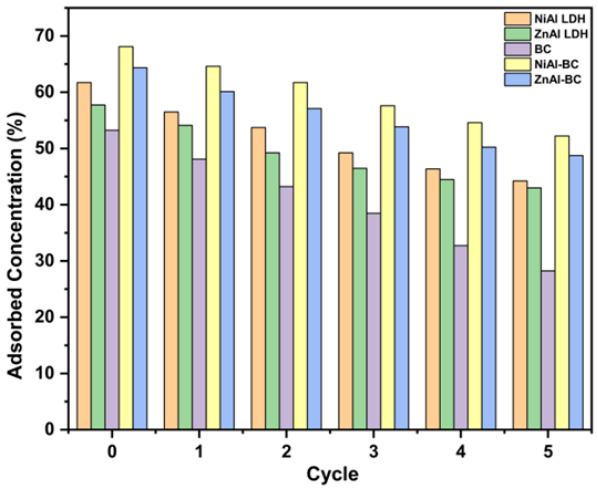

Figure 8. Reusability of adsorbent materials.

3.6 Reusability of Adsorbents

Figure 8 shows the effectiveness of an adsorbent for reuse. The graph obtained showed the reusability process up to five cycles, where NiAl-BC had the highest adsorption percentage with a percentage of 68.10% and experienced an insignificant decrease in the fifth cycle, from 68.10% to 52.23%. The next highest adsorption percentages were ZnAl-BC, NiAl LDH, ZnAl LDH, and BC, which each had adsorption percentages of 64.35, 61.73, 57.73, 53.23%. Also, as the number of reusability cycles went up, the ability to absorb dropped. In the fifth cycle, it dropped by 15.62, 17.50, 14.75, and 24.99%, respectively.

3.7 Mechanism of Phenol Adsorption

The interactions that occur in phenol adsorption can be seen in Figure 9 which shows the FT-IR analysis after adsorption. According to Haydari *et al*. [57] the common mechanisms that occur in phenol adsorption are electrostatic interactions, hydrogen bond interactions, and π-π electron pair interactions. In Figure 9 it can be seen that there has been a shift in several wavenumbers including the wavenumber 1627 cm^{-1} which indicates the occurrence of π-π interactions in C=C aromatic biochar with phenol aromatic rings. At wavenumber 1049 cm^{-1} there is a shift indicating an electrostatic interaction. The electrostatic interaction is also evidenced by a shift in the metal-oxide wavenumber region where the positive charge on LDH binds to the negative charge on the phenol according to pH<pHpzc.

Table 5. Adsorption thermodynamic parameter.

Adsorbent	Concentration (mg/L)	ΔH (kJ/mol)	ΔS (kJ/mol)	ΔG (kJ/mol)				
				303 K	313 K	323 K	333 K	343 K
NiAl LDH	30	17.989	0.068	-2.703	-3.386	-4.069	-4.752	-5.435
ZnAl LDH	30	13.44	0.052	-2.184	-2.700	-3.216	-3.731	-4.247
BC	30	15.456	0.061	-3.061	-3.672	-4.283	-4.894	-5.505
NiAl-BC	30	20.467	0.081	-3.942	-4.748	-5.554	-6.359	-7.165
ZnAl-BC	30	13.676	0.055	-3.005	-3.556	-4.106	-4.657	-5.207

In addition, there is also a hydrogen bond interaction that occurs in phenol adsorption which is marked by a shift at wavenumber 3448 cm^{-1}. The adsorption mechanism that occurs in phenol adsorption can be seen in Figure 10.

4. Conclusion

In this study, NiAl LDH and ZnAl LDH composites were successfully prepared using XRD, FTIR, and BET characterization techniques. NiAl LDH and ZnAl LDH have an optimal pH of 3, NiAl-BC and ZnAl-BC have an optimal pH of 5, and biochar has an optimal pH of 7. The kinetics model was PSO-based, whereas the isotherm model was Freundlich-based. NiAl LDH, ZnAl LDH, BC, NiAl-BC, and ZnAl-BC had maximal adsorption capacities of 45.87, 37.17, 35.33, 74.62, and 52.91 mg/g, respectively. The recurrent usage of the material demonstrates that NiAl-BC has a superior ability, which is not significantly diminished by the fifth cycle. Then ZnAl-BC, NiAl LDH, ZnAl LDH, and BC follow.

Acknowledgement

Author acknowledges the help and instrumental analysis of the Research Center of Inorganic Materials and Coordination Complexes, Universitas Sriwijaya for assisting in the completion of this study.

CRediT Author Statement

Author Contributions: **A. Amri**: Conceptualization, Investigation, Writing–Original draft, Software; **R. Rezonsi**: Investigation, Formal analysis, Resources; **N. Ahmad**: Visualization, Formal Analysis; **T. Taher**: Meth-

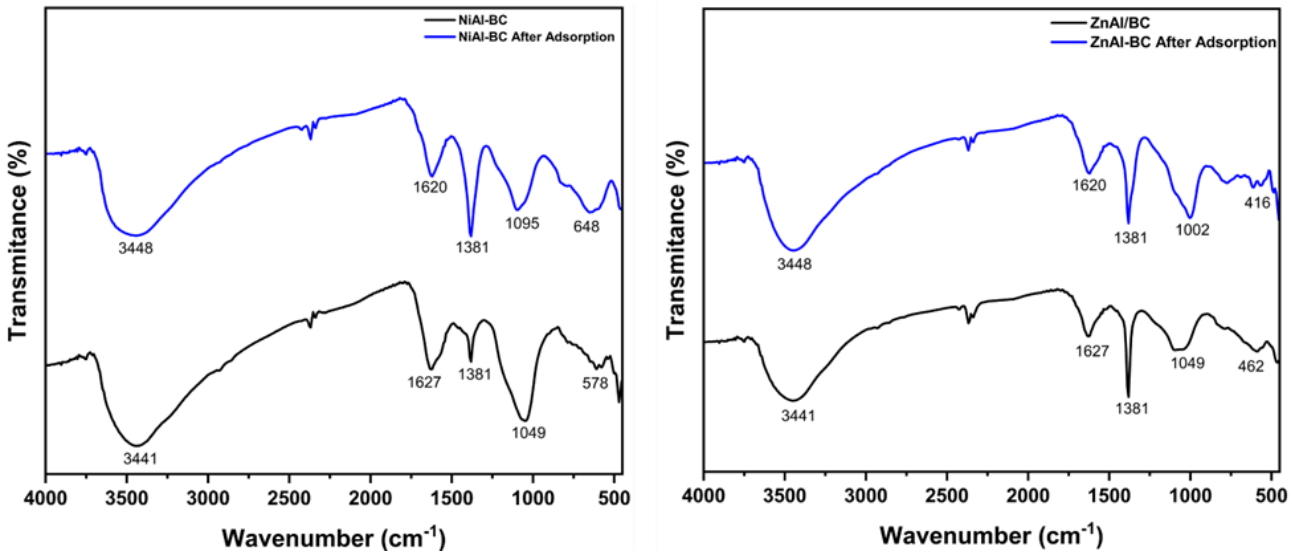

Figure 9. Fourier transfer infra-red spectrum of NiAl-BC and ZnAl-BC adsorbents after adsorption.

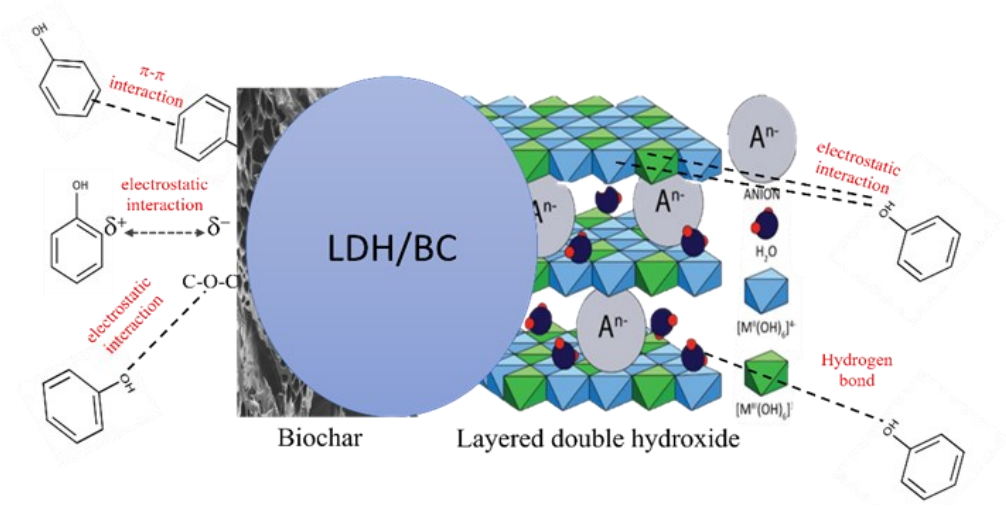

Figure 10. Phenol adsorption mechanism.

odology, Data Curation, Visualization; **N. R. Palapa**: Formal analysis , Visualization; R. Mohadi: Validation, Data Curation; **A. Lesbani**: Methodology, Conceptualization, Funding acquisition, Writing–review & editing, Supervision.

References

[1] Clover, D.E., de O. Jayme, B., Hall, B.L., Follen, S. (2013). The Nature of Transformation: Environmental Adult Education. *The Nature of Transformation: Environmental Adult Education*, 3, 1–128. DOI: 10.1007/978-94-6209-146-7.

[2] Gami, A.A., Shukor, M.Y., Khalil, K.A., Dahalan, F. A., Khalid, A., Ahmad, S.A. (2014). Phenol and its toxicity. *Journal of Environmental Microbiology and Toxicology*, 2(1), 11-24. DOI: 10.54987/jemat.v2i1.89

[3] Khan, D., Kuntail, J., Sinha, I. (2022). Mechanism of phenol and p-nitrophenol adsorption on kaolinite surface in aqueous medium: A molecular dynamics study. *Journal of Molecular Graphics and Modelling*, 116, 108251. DOI: 10.1016/j.jmgm.2022.108251.

[4] Mishra, P., Singh, K., Dixit, U. (2021). Adsorption, kinetics and thermodynamics of phenol removal by ultrasound-assisted sulfuric acid-treated pea (Pisum sativum) shells. *Sustainable Chemistry and Pharmacy*, 22, 100491. DOI: 10.1016/j.scp.2021.100491.

[5] Cao, Y., Wang, Y., Zhou, F., Huang, J., Xu, M. (2022). Acylamino-functionalized hyper-crosslinked polymers for efficient adsorption removal of phenol in aqueous solution. *Separation and Purification Technology*, 303, 122229. DOI: 10.1016/j.seppur.2022.122229.

[6] Wang, B., Wu, K., Liu, T., Luan, H., Xue, K., Liu, Y., Niu, Y. (2023). International Journal of Biological Macromolecules Synthesis of hyperbranched polyamine dendrimer / chitosan / silica composite for efficient adsorption of Hg (II). *International Journal of Biological Macromolecules*, 230, 123135. DOI: 10.1016/j.ijbiomac.2023.123135.

[7] Jain, M., Khan, S.A., Sahoo, A., Dubey, P., Pant, K.K., Ziora, Z.M., Blaskovich, M.A.T. (2022). Statistical evaluation of cow-dung derived activated biochar for phenol adsorption: Adsorption isotherms, kinetics, and thermodynamic studies. *Bioresource Technology*, 352, 127030. DOI: 10.1016/j.biortech.2022.127030.

[8] Chaari, I., Touil, A., Medhioub, M. (2021). Adsorption-desorption of phenolic compounds from olive mills wastewater using Tunisian natural clay. *Chinese Journal of Chemical Engineering*, 40, 287–292. DOI: 10.1016/j.cjche.2020.12.020.

[9] Tshemese, S.J., Mhike, W., Tichapondwa, S.M. (2021). Adsorption of phenol and chromium (VI) from aqueous solution using exfoliated graphite: Equilibrium, kinetics and thermodynamic studies. *Arabian Journal of Chemistry*, 14(6), 103160. DOI: 10.1016/j.arabjc.2021.103160.

[10] Lupa, L., Cocheci, L., Pode, R., Hulka, I. (2018). Phenol adsorption using Aliquat 336 functionalized Zn-Al layered double hydroxide. *Separation and Purification Technology*, 196, 82–95. DOI: 10.1016/j.seppur.2017.10.003.

[11] Xie, X.Z., Xu, L., Pan, Y., Mi, J.X. (2022). Facile synthesis of rose-like composites of zeolites and layered double hydroxides: Growth mechanism and enhanced properties. *Chemosphere*, 309(P2), 136741. DOI: 10.1016/j.chemosphere.2022.136741.

[12] Mahjoubi, F.Z., Khalidi, A., Abdennouri, M., Barka, N. (2017). Zn–Al layered double hydroxides intercalated with carbonate, nitrate, chloride and sulphate ions: Synthesis, characterisation and dye removal properties. *Journal of Taibah University for Science*, 11(1), 90–100. DOI: 10.1016/j.jtusci.2015.10.007.

[13] Siregar, P.M.S.B.N., Wijaya, A., Amri, Nduru, J.P., Hidayati, N., Lesbani, A., Mohadi, R. (2022). Layered Double Hydroxide/C (C = Humic Acid; Hydrochar) As Adsorbents of Cr(VI). *Science and Technology Indonesia*, 7(1), 41–48. DOI: 10.26554/sti.2022.7.1.41-48.

[14] Jiang, Y., Shen, Z., Tang, C.S., Shi, B. (2023). Synthesis and application of waste-based layered double hydroxide: A review. *Science of the Total Environment*, 903, 166245. DOI: 10.1016/j.scitotenv.2023.166245.

[15] Mishra, G., Dash, B., Pandey, S. (2018). Layered double hydroxides: A brief review from fundamentals to application as evolving biomaterials. *Applied Clay Science*, 153, 172–186. DOI: 10.1016/j.clay.2017.12.021.

[16] Figueiredo, M.P., Suarez, E.D., Petrilli, H.M., Leroux, F., Taviot-Guého, C., Constantino, V.R.L. (2022). Limiting content of trivalent iron to form organic-inorganic single-phase layered double hydroxides hybrids by co-precipitation. *Applied Clay Science*, 228, 106642. DOI: 10.1016/j.clay.2022.106642.

[17] Gouasmia, A., Zouaoui, E., Mekkaoui, A.A., Haddad, A., Bousba, D. (2022). Highly efficient photocatalytic degradation of malachite green dye over copper oxide and copper cobaltite photocatalysts under solar or microwave irradiation. *Inorganic Chemistry Communications*, 145, 110066. DOI: 10.1016/j.inoche.2022.110066.

[18] Siregar, P.M.S.B.N., Palapa, N.R., Wijaya, A., Fitri, E.S., Lesbani, A. (2021). Structural Stability of Ni/Al Layered Double Hydroxide Supported on Graphite and Biochar Toward Adsorption of Congo Red. *Science and Technology Indonesia*, 6(2), 85–95. DOI: 10.26554/STI.2021.6.2.85-95.

[19] Ahmad, N., Suryani, F., Royani, I., Lesbani, A. (2023). Results in Chemistry Charcoal activated as template Mg / Al layered double hydroxide for selective adsorption of direct yellow on anionic dyes. *Results in Chemistry*, 5, 100766. DOI: 10.1016/j.rechem.2023.100766.

[20] Yang, B., Liu, J., Liu, Z., Wang, Y., Cai, J., Peng, L. (2019). Preparation of chitosan/Co-Fe-layered double hydroxides and its performance for removing 2,4-dichlorophenol. *Environmental Science and Pollution Research*, 26(4), 3814–3822. DOI: 10.1007/s11356-018-3886-x.

[21] dos Santos Lins, P.V., Henrique, D.C., Ide, A.H., de Paiva e Silva Zanta, C.L., Meili, L. (2019). Evaluation of caffeine adsorption by MgAl-LDH/biochar composite. *Environmental Science and Pollution Research*, 26(31), 31804–31811. DOI: 10.1007/s11356-019-06288-3.

[22] Pathy, A., Pokharel, P., Chen, X., Balasubramanian, P., Chang, S.X. (2023). Science of the Total Environment Activation methods increase biochar ' s potential for heavy-metal adsorption and environmental remediation : A global meta-analysis. *Science of the Total Environment*, 865(August 2022), 161252. DOI: 10.1016/j.scitotenv.2022.161252.

[23] Gao, Y., Fang, Z., Lin, W., Chen, H., Bhatnagar, A., Li, J., Xie, Y., Bao, Y., Chen, J., Zhao, H., Meng, J., Chen, W., Wang, H. (2023). Large-flake graphene-modified biochar for the removal of bisphenol S from water: rapid oxygen escape mechanism for synthesis and improved adsorption performance. *Environmental Pollution*, 317, 120847. DOI: 10.1016/j.envpol.2022.120847.

[24] Normah, N., Palapa, N.R., Taher, T., Mohadi, R., Utami, H.P., Lesbani, A. (2021). The Ability of Composite Ni/Al-Carbon Based Material Toward Readsorption of Iron(II) in Aqueous Solution. *Science and Technology Indonesia*, 6(3), 156–165. DOI: 10.26554/sti.2021.6.3.156-165.

[25] Mahgoub, S.M., Shehata, M.R., Zaher, A., Abo El-Ela, F.I., Farghali, A., Amin, R.M., Mahmoud, R. (2022). Cellulose-Based Activated Carbon/Layered Double Hydroxide for Efficient Removal of Clarithromycin Residues and Efficient Role in the Treatment of Stomach Ulcers and Acidity Problems. *International Journal of Biological Macromolecules*, 215, 705–728. DOI: 10.1016/j.ijbiomac.2022.06.136.

[26] Hoang, L.P., Nguyen, T.M.P., Van, H.T., Yılmaz, M., Hoang, T.K., Nguyen, Q.T., Vi, T.M.H., Nga, L.T.Q. (2022). Removal of Tetracycline from aqueous solution using composite adsorbent of ZnAl layered double hydroxide and bagasse biochar. *Environmental Technology and Innovation*, 28, 102914. DOI: 10.1016/j.eti.2022.102914.

[27] Liao, W., Zhang, X., Shao, J., Yang, H., Zhang, S., Chen, H. (2022). Simultaneous Removal of Cadmium and Lead by Biochar Modified with Layered Double Hydroxide. *Fuel Processing Technology*, 235, 107389. DOI: 10.1016/j.fuproc.2022.107389.

[28] Wang, X., Chen, A., Chen, B., Wang, L. (2020). Adsorption of phenol and bisphenol A on river sediments: Effects of particle size, humic acid, pH and temperature. *Ecotoxicology and Environmental Safety*, 204, 111093. DOI: 10.1016/j.ecoenv.2020.111093.

[29] Alminderej, F.M., Younis, A.M., Albadri, A.E.A.E., El-Sayed, W.A., El-Ghoul, Y., Ali, R., Mohamed, A.M.A., Saleh, S.M. (2022). The superior adsorption capacity of phenol from aqueous solution using Modified Date Palm Nanomaterials: A performance and kinetic study. *Arabian Journal of Chemistry*, 15(10), 104120. DOI: 10.1016/j.arabjc.2022.104120.

[30] Yılmaz, Ş. (2022). Facile synthesis of surfactant-modified layered double hydroxide magnetic hybrid composite and its application for bisphenol A adsorption: Statistical optimization of operational variables. *Surfaces and Interfaces*, 32, 102171. DOI: 10.1016/j.surfin.2022.102171.

[31] Mallakpour, S., Azadi, E., Dinari, M. (2023). Removal of cationic and anionic dyes using Ca-alginate and Zn-Al layered double hydroxide/metal-organic framework. *Carbohydrate Polymers*, 301(PB), 120362. DOI: 10.1016/j.carbpol.2022.120362.

[32] Prakongkep, N., Gilkes, R.J., Wiriyakitnateekul, W., Duangchan, A., Darunsontaya , T. (2013). The effects of pyrolysis conditions on the chemical and physical properties of rice husk biochar. *International Journal of Material Science (IJMSCI)*, 3(3), 97–103.

[33] Rashed, S.H., Abd-Elhamid, A.I., Abdalkarim, S.Y.H., El-Sayed, R.H., El-Bardan, A.A., Soliman, H.M.A., Nayl, A.A. (2022). Preparation and Characterization of Layered-Double Hydroxides Decorated on Graphene Oxide for Dye Removal from Aqueous Solution. *Journal of Materials Research and Technology*, 17, 2782–2795. DOI: 10.1016/j.jmrt.2022.02.040.

[34] Santosa, S.J., Krisbiantoro, P.A., Minh Ha, T.T., Thanh Phuong, N.T., Gusrizal, G. (2021). Composite of magnetite and Zn/Al layered double hydroxide as a magnetically separable adsorbent for effective removal of humic acid. *Colloids and Surfaces A: Physicochemical and Engineering Aspects*, 614, 126159. DOI: 10.1016/j.colsurfa.2021.126159.

[35] Ravuru, S.S., Jana, A., De, S. (2019). Synthesis of NiAl- layered double hydroxide with nitrate intercalation: Application in cyanide removal from steel industry effluent. *Journal of Hazardous Materials*, 373, 791–800. DOI: 10.1016/j.jhazmat.2019.03.122.

[36] Zhang, P., O'Connor, D., Wang, Y., Jiang, L., Xia, T., Wang, L., Tsang, D.C.W., Ok, Y.S., Hou, D. (2020). A green biochar/iron oxide composite for methylene blue removal. *Journal of Hazardous Materials*, 384, 121286. DOI: 10.1016/j.jhazmat.2019.121286.

[37] Meili, L., Lins, P. V., Zanta, C.L.P.S., Soletti, J.I., Ribeiro, L.M.O., Dornelas, C.B., Silva, T.L., Vieira, M.G.A. (2019). MgAl-LDH/Biochar composites for methylene blue removal by adsorption. *Applied Clay Science*, 168, 11–20. DOI: 10.1016/j.clay.2018.10.012.

[38] Missau, J., Bertuol, D.A., Tanabe, E.H. (2021). Highly efficient adsorbent for removal of Crystal Violet Dye from Aqueous Solution by CaAl/LDH supported on Biochar. *Applied Clay Science*, 214, 106297. DOI: 10.1016/j.clay.2021.106297.

[39] Zubair, M., Aziz, H.A., Ihsanullah, I., Ahmad, M.A., Al-Harthi, M.A. (2022). Engineered biochar supported layered double hydroxide-cellulose nanocrystals composite-: Synthesis, characterization and azo dye removal performance. *Chemosphere*, 307(P4), 136054. DOI: 10.1016/j.chemosphere.2022.136054.

[40] Jadam, M.L., Sarijo, S.H., Jubri, Z. (2022). Synthesis and Characterisation of Layered Double Hydroxides with Varying Divalent Metal Cations: Mg2+, Zn2+, Ca2+. *Materials Today: Proceedings*, 66, 4015–4019. DOI: 10.1016/j.matpr.2022.05.162.

[41] Li, Y., Bi, H.Y., Mao, X.M., Liang, Y.Q., Li, H. (2018). Adsorption behavior and mechanism of core–shell magnetic rhamnolipid–layered double hydroxide nanohybrid for phenolic compounds from heavy metal–phenolic pollutants. *Applied Clay Science*, 162, 230–238. DOI: 10.1016/j.clay.2018.06.013.

[42] Khedri, D., Hessam, A., Moniri, E., Ahmad, H. (2022). Efficient removal of phenolic contaminants from wastewater samples using functionalized graphene oxide with thermosensitive polymer : Adsorption isotherms , kinetics , and thermodynamics studies. *Surfaces and Interfaces*, 35, 102439. DOI: 10.1016/j.surfin.2022.102439.

[43] Niaei, H.A., Rostamizadeh, M. (2020). Adsorption of metformin from an aqueous solution by Fe-ZSM-5 nano-adsorbent: Isotherm, kinetic and thermodynamic studies. *Journal of Chemical Thermodynamics*, 142, 106003. DOI: 10.1016/j.jct.2019.106003.

[44] Budnyak, T.M., Vlasova, N.N., Golovkova, L.P., Slabon, A., Tertykh, V.A. (2019). Bile acids adsorption by chitoan-fumed silica enterosorbent. *Colloids and Interface Science Communications*, 32, 100194. DOI: 10.1016/j.colcom.2019.100194.

[45] Dehmani, Y., Khalki, O. El, Mezougane, H., Abouarnadasse, S. (2021). Comparative study on adsorption of cationic dyes and phenol by natural clays. *Chemical Data Collections*, 33, 100674. DOI: 10.1016/j.cdc.2021.100674.

[46] Keshvardoostchokami, M., Majidi, M., Zamani, A., Liu, B. (2021). Adsorption of phenol on environmentally friendly Fe3O4/ chitosan/ zeolitic imidazolate framework-8 nanocomposite: Optimization by experimental design methodology. *Journal of Molecular Liquids*, 323, 115064. DOI: 10.1016/j.molliq.2020.115064.

[47] Mukherjee, M., Goswami, S., Banerjee, P., Sengupta, S., Das, P., Banerjee, P.K., Datta, S. (2019). Ultrasonic assisted graphene oxide nanosheet for the removal of phenol containing solution. *Environmental Technology and Innovation*, 13, 398–407. DOI: 10.1016/j.eti.2016.11.006.

[48] Liu, X., Tu, Y., Liu, S., Liu, K., Zhang, L., Li, G., Xu, Z. (2021). Adsorption of ammonia nitrogen and phenol onto the lignite surface: An experimental and molecular dynamics simulation study. *Journal of Hazardous Materials*, 416, 125966. DOI: 10.1016/j.jhazmat.2021.125966.

[49] Yousef, R.I., El-Eswed, B., Al-Muhtaseb, A.H. (2011). Adsorption characteristics of natural zeolites as solid adsorbents for phenol removal from aqueous solutions: Kinetics, mechanism, and thermodynamics studies. *Chemical Engineering Journal*, 171(3), 1143–1149. DOI: 10.1016/j.cej.2011.05.012.

[50] da Gama, B.M.V., do Nascimento, G.E., Sales, D.C.S., Rodríguez-Díaz, J.M., de Menezes Barbosa, C.M.B., Duarte, M.M.M.B. (2018). Mono and Binary Component adsorption of phenol and cadmium using adsorbent derived from peanut shells. *Journal of Cleaner Production*, 201, 219–228. DOI: 10.1016/j.jclepro.2018.07.291.

[51] Tamang, M., Paul, K.K. (2022). Adsorptive treatment of phenol from aqueous solution using chitosan/calcined eggshell adsorbent: Optimization of preparation process using Taguchi statistical analysis. *Journal of the Indian Chemical Society*, 99(1), 100251. DOI: 10.1016/j.jics.2021.100251.

[52] Nakhjiri, M.T., Marandi, G.B., Kurdtabar, M. (2021). Preparation of magnetic double network nanocomposite hydrogel for adsorption of phenol and p-nitrophenol from aqueous solution. *Journal of Environmental Chemical Engineering*, 9(2), 105039. DOI: 10.1016/j.jece.2021.105039.

[53] Dehmani, Y., Lgaz, H., Alrashdi, A.A., Lamhasni, T., Abouarnadasse, S., Chung, I.M. (2021). Phenol adsorption mechanism on the zinc oxide surface: Experimental, cluster DFT calculations, and molecular dynamics simulations. *Journal of Molecular Liquids*, 324, 114993. DOI: 10.1016/j.molliq.2020.114993.

[54] Mandal, A., Mukhopadhyay, P., Das, S.K. (2019). The study of adsorption efficiency of rice husk ash for removal of phenol from wastewater with low initial phenol concentration. *SN Applied Sciences*, 1(2) DOI: 10.1007/s42452-019-0203-3.

[55] Ha, N.T.T., Thao, H.T., Ha, N.N. (2022). Physisorption and chemisorption of CO2 on Fe-MIL-88B derivatives: Impact of the functional groups on the electronic properties and adsorption tendency - A theoretical investigation. *Journal of Molecular Graphics and Modelling*, 112, 108124. DOI: 10.1016/j.jmgm.2022.108124.

[56] Shin, J., Kwak, J., Kim, S., Son, C., Lee, Y.G., Baek, S., Park, Y., Chae, K.J., Yang, E., Chon, K. (2022). Facilitated physisorption of ibuprofen on waste coffee residue biochars through simultaneous magnetization and activation in groundwater and lake water: Adsorption mechanisms and reusability. *Journal of Environmental Chemical Engineering*, 10(3), 107914. DOI: 10.1016/j.jece.2022.107914.

[57] Haydari, I., Aziz, K., Ouazzani, N., Mandi, L., Aziz, F. (2023). Green synthesis of reduced graphene oxide and their use on column adsorption of phenol from olive mill wastewater. *Process Safety and Environmental Protection*, 170, 1079–1091. DOI: 10.1016/j.psep.2022.12.086.